Structural Eng./Earthquake Eng., JSCE, Vol. 14, No. 2, 161s—173s, 1997 July
(J. Struct. Mech. Earthquake Eng., JSCE, No. 570/ I —40)

CONTACT PROBLEMS AND STRESS DISTRIBUTION OF A PIN-CONNECTION DETAIL

Harukazu OHASHI[1], Chitoshi MIKI[2] and Shuichi ONO[3]

[1] Member of JSCE, Dr. of Eng., Design Department, Honshu-Shikoku Bridge Authority (4-1-22 Onoedori, Chuo-ku, Kobe-shi, Hyogo 615)
[2] Fellow member of JSCE, Dr. of Eng., Professor, Dept. of Civil Eng., Tokyo Institute of Technology (2-12-1 Ohokayama, Meguro-ku, Tokyo 152)
[3] Member of JSCE, M.S., Japan Construction Method and Machinery Research Institute (3154 Ohbuchi, Fuji-shi, Shizuoka 417)

This paper presents the force transfer mechanism and the fatigue performance of a pin-connection anchor of hanger for a box-type suspension bridge. Static loading tests were conducted using a full scale specimen, and contact pressure distribution and pin bending stress were measured under the design ordinary and wind loading conditions. In the subsequent cyclic loading tests, it was found that fatigue cracks occurred from seal weld at pinhole. Finite element analysis showed contact pressure distribution and the stress at welds of anchor plate and doubling plates.

Key Words : *pin-connection anchor, hanger, force transfer mechanism, fatigue performance, doubling plates, contact pressure*

1. INTRODUCTION

For suspension bridges in the Honshu-Shikoku Bridges, a flexible rope (CFRC : Center Fit Rope Core) has been used as hangers and it is saddled from cable band and the socket is fixed by bearing to the girder (**Fig.1-(a)**). However, pin anchor to connect hanger ropes to stiffening girder and cable bands has been greatly desired especially for box-type suspension bridges because this simplifies the connection detail (**Fig.1-(b)**). By using a pin-connection anchor, the hanger can be basically treated as a straight member, thus extending application of different ropes and cables. For example, the adoption of a parallel-wire cable (PWS) with high tensile strength can decrease the number and/or diameter which may result in a simplification of connection detail at both the stiffening girder and the cable band. Its high fatigue performance will prolong the life. Further polyethylene extrusion technique developed for stay-cables of cable-stayed bridges can be used for hangers, which will increase reliability against corrosion. The polyethylene tube covers up to the mouth of socket and can deform as hanger deforms by bending due to wind loading oscillation.

A pin-connection anchor has been used in actual suspension bridges, including the 118-year old Brooklyn bridge and modern bridges such as Severn and Humber bridges in the United Kingdom. However, there is no detailed information on designing anchor structures.

In order to investigate the force transfer mechanism and to examine the fatigue strength of a pin-connection anchor, static and cyclic loading tests were conducted on a full scale specimen. Finally, the contact condition and stress distribution at anchor, doubling plates and welds were analyzed by elastic finite element method.

2. A PIN-CONNECTION ANCHOR DETAIL AND RELATED ROBLEMS

Socket of a hanger rope is pin-connected to the anchor (**Fig.2**). Under the design ordinary loading condition, vertical force from hanger acts to the pin-connection anchor. Live load component of approximately 20 to 30% of total tensile force respectively acts on the anchor.

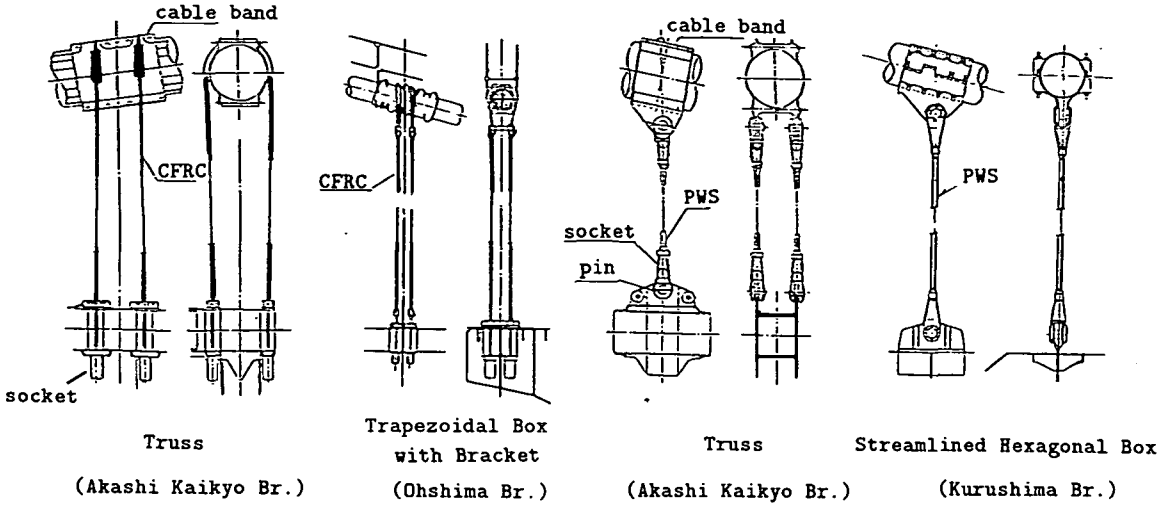

(a) Type of the socket fixed by bearing

(b) Type of the socket fixed using pin

Fig.1 Type of anchor for hanger

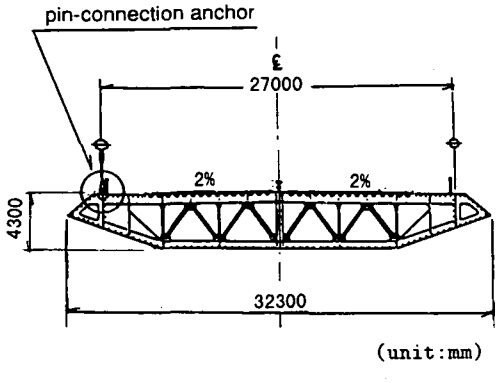

Fig.2 Pin-connection detail for a box-type stiffening girder

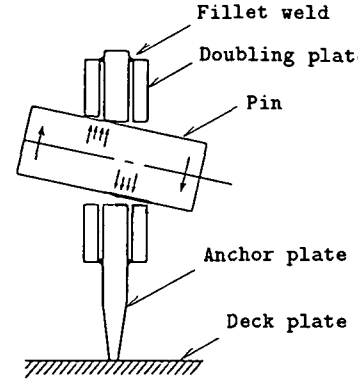

Fig.3 Inclination of pin axis during the wind loading conditions (schematic illustration)

Under the design wind loading condition, however, a lateral force also acts at the pin-connection anchor as a result of relative horizontal displacement between the main cables and the stiffening girder. The calculated maximum inclination angle of the hanger is 3.2 degrees for a 1,000m span streamlined-box-type suspension bridge. The gap between the pin and the pinhole allows the inclination of pin axis under wind loading condition, as shown in **Fig.3**.

Major problems discussed here are summarized below.

(1) The anchor plate is mostly reinforced by doubling plates for supplementing the lack of sectional area due to the pinhole. Stress distribution of the eyebar subjected to tensile force which acts at pinhole was studied by J.Beke[1]. Later by Suzuki et al.[2], stress distribution around pinhole for seismic restrainer was analyzed by use of boundary element method.

Also the fatigue strength of the eyebar was fully investigated after the collapse of Point Pleasant Bridge in 1957[3]. However, the design of the anchor reinforced by doubling plates has not been studied.

(2) The doubling plates are welded to the anchor plate along the outer periphery of doubling plates. The weld design has to be established.

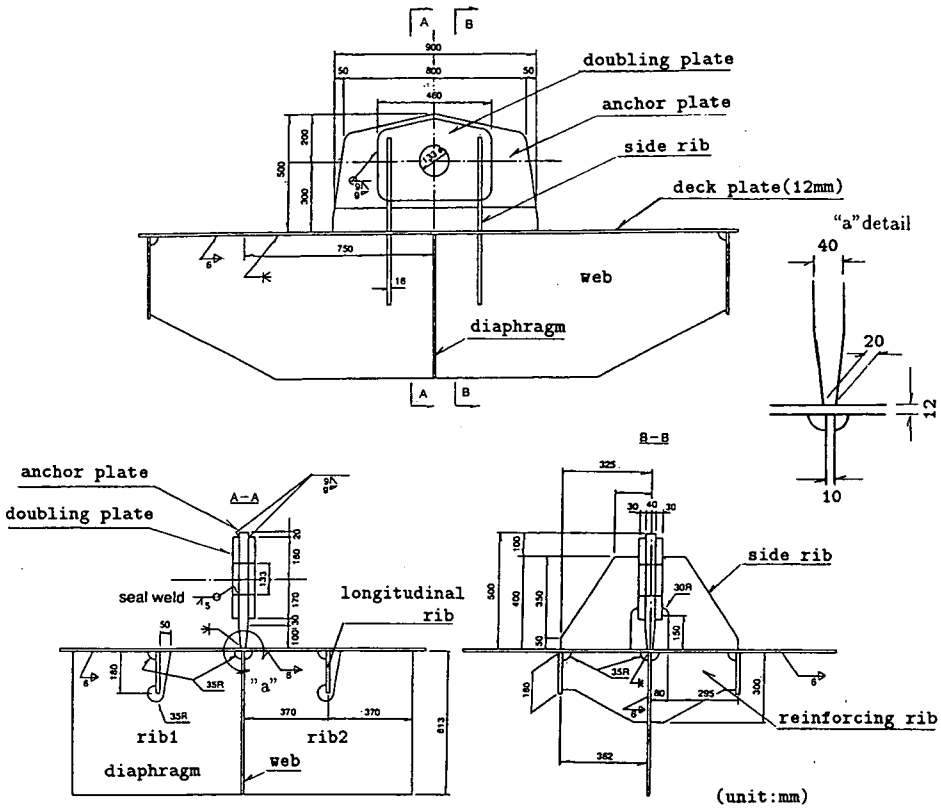

Fig.4 Structural detail of a specimen

Table 1 Mechanical and chemical properties of steels used

parts	steel	mechanical properties			chemical composition (%)										
		Yp	Ts	EL	C	Si	Mn	P	S	Cu	Ni	Cr	Mo	Nb	Ceq
		(N/mm^2)	(N/mm^2)	(%)	×100			×1000		×	×10000		×100		
pin	SCM435	922	1,020	18	35	25	78	16	18	17	8	111	16		
deck	SM400A	312	452	30	15	18	65	14	5						
anchor	SM490YB	372	538	30	17	44	133	19	5	1					41
doubling	SM490YB	408	554	28	17	45	142	13	2	1				2	42
web	SM490YA	421	566	26	17	44	132	20	7	1					41
diaphragm	SS400	292	443	28	16	18	66	16	8						

Draft were obtained from mill sheets.

(3) In order to prevent corrosion of the pinhole, seal weld is often conducted at the gap between the anchor plate and the doubling plate. Stress condition at the seal weld, not only the fillet weld, have to be investigated.

(4) In design practice, the pin is designed to bear contact pressure (bearing stress) and bending moment, assuming the angle of contact area and the pressure distribution. In many designs, the contact angle is set at 90 degrees and pressure is a cosine distribution[4]. These assumptions must be verified.

3. TESTING METHOD

(1) Test Specimen

A full-sized model of the pin-connection anchor was fabricated as a test specimen. **Fig.4** shows the detail of the pin-connection anchor. The pinhole diameter is 133mm and the pin is 130mm. SM490Y steel was used for the anchor and a chromium molybdenum steel, SCM435 for the pin. The Brinell hardness is about 150 for the plate and is 269～331 for the pin. **Table 1** shows the mechanical and chemical properties of steels used for the specimen.

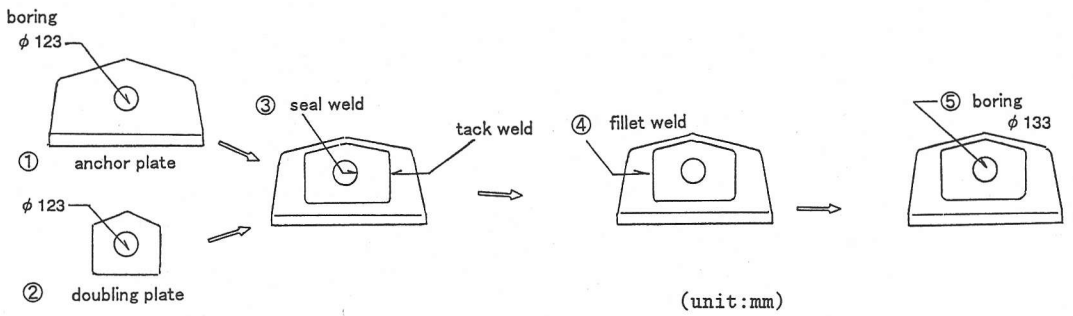

Fig.5 Welding procedure

In order to exclude the unknown factors in the fabrication process, the fabrication method and welding procedures were the same as in the actual manufacturing plan (cf. **Fig.5**). The anchor plate was welded directly on the deck plate by full penetration weld. Seal weld was performed inside the pinhole. After welding, final grinding of pinhole work was conducted.

(2) Static and cyclic loading tests

Vertical load was applied to the specimen through a cable fixed to a large-scale fatigue testing machine with 5,900kN static and 3,900kN dynamic loading capacity (**Fig.6**). For the wind loading condition, base of the specimen was set at the maximum design inclination angle of 3.2 degrees for a 1,000m span box-type suspension bridge.

Cyclic load was then applied to the same specimen, beginning with design ordinary loading condition. After two million repetitions, all fatigue cracks were retrofitted by welding. Cyclic loads were then applied to the same specimen for design wind loading condition.

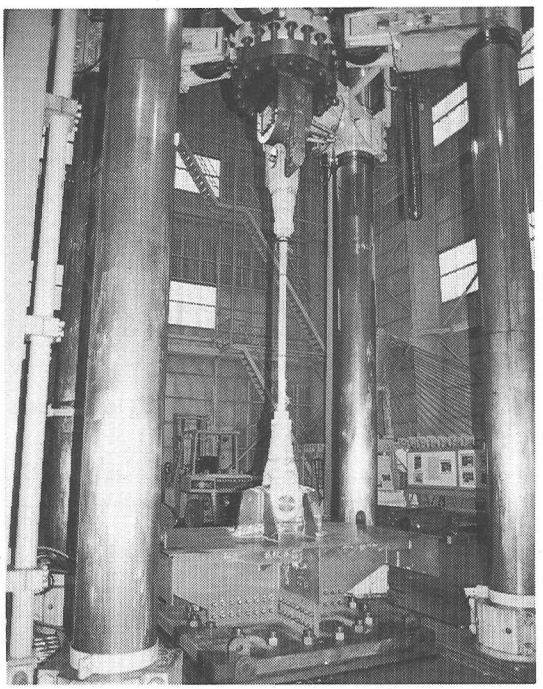

Fig.6 Test set-up

4. STATIC LOADING TEST RESULT

Static load was applied to the specimen and strain was measured at the anchor plate, the doubling plate, and the reinforcing structure inside the box girder. Strain measurement of the pin was made by attaching strain gauges in 2mm deep gutters. The contact area was simultaneously measured by use of pressure scale paper (maximum contact pressure to be measured is 700 kgf/cm^2). The scale pressure paper was inserted in the pinhole and then vertical load was applied.

Fig.7 shows the measured principal stresses at the anchor structure, both under the ordinary and the wind loading conditions.

Also side ribs for the anchor plate which was designed to resist lateral force carried tensile stress even at vertical loading.

Under the wind loading condition, difference of stresses can be noticed between the both faces of the doubling plates due to the eccentric loading (see **Fig.7-(b)**).

Fig.8 shows the contact area between the pin and the pinhole measured by the pressure scale paper of 0.2mm in thickness. Contact area was almost uniform along the pin axis. Discontinuity of contact area at the interface between the anchor and the doubling plate found in the reference 5 was not observed in this test. By increasing vertical load, the contact region was extended to the periphery and the contact area increased almost linearly (**Fig.9**).

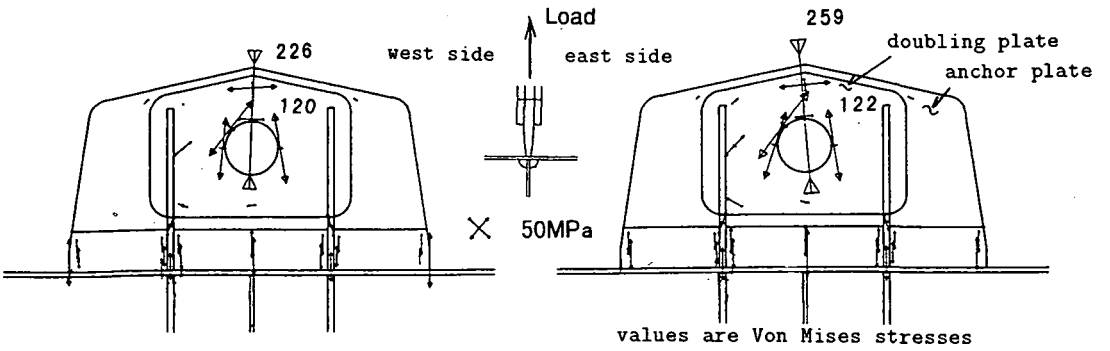

(a) Ordinary loading condition

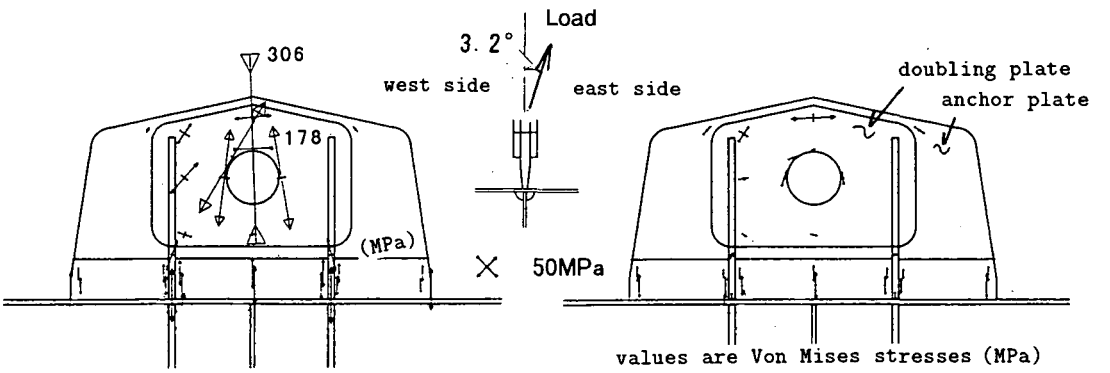

(b) Wind loading condition

Fig.7 Principal stress distribution at anchor structure

Under the wind loading condition, the contact area was concentrated at either of the doubling plates due to inclination of the pin. And, the pin was only in contact on the upper face of the pinhole. This implies that high shear stress acted at the seal weld which connect the anchor and doubling plates.

Pin stresses were measured at the top and the bottom of the pin. **Fig.10** showed the bending stress of the pin at different locations. The center of moment of inertia was above the neutral axis.

Deformation of the pinhole was measured after total of four million repetition of the cyclic loading test with two million each under the ordinary and the wind loading conditions. As shown in **Fig.11**, the residual deformation of the pinhole was 0.7mm at its left edge.

5. CYCLIC LOADING TEST RESULT

Table 2 shows applied loading amplitude. Under the ordinary loading condition, the minimum load was set to the tensile force due to the design dead load and the loading amplitude was set to the tensile force due to live load.

The largest loading amplitude for the wind loading condition might be approximately 15% of design wind load considering a gust component. In the test, however, design wind load was applied considering the test duration available.

Under the ordinary loading condition, there was no crack found at the welds between the anchor and doubling plates. However, when the pin was removed after completion of all tests including wind loading condition, cracks were found at the seal weld on the pinhole surface(**Fig.12**). Those cracks were located at high stress bearing zone and the cracks were extended along the weld line and finally to the anchor plate. The number of cycles at the initiation of the cracks could not be confirmed from the fractured surface.

Depth of penetration of seal weld was measured from the fractured surfaces (**Fig.13**). Penetration depth varied from 7.5mm to almost zero.

Both cracks were initiated near the places where

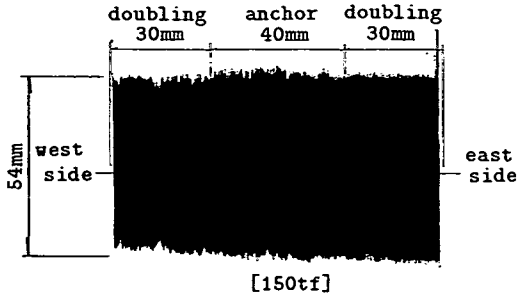

(a) Ordinary loading condition

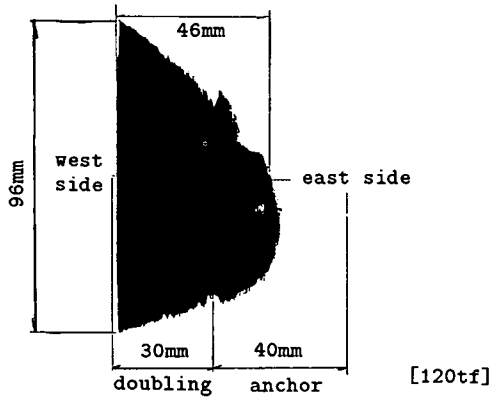

(b) Wind loading condition

Fig.8 Contact surface measured by a pressure scale paper

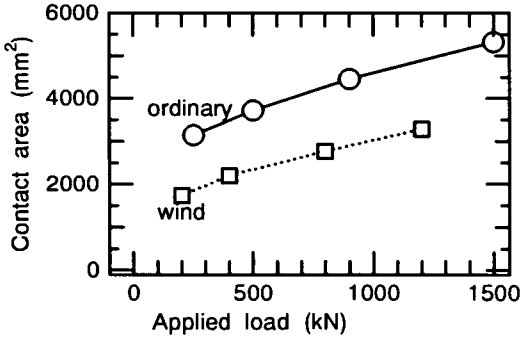

Fig.9 Measured contact area with relation to applied loads

there was little penetration.

6. ANALYSIS AND EVALUATION

(1) Finite element model

After the tests, stress analysis by elastic finite element method was conducted on the half model

Table 2 Loading condition

Items	Loading condition	
	Ordinary	Wind
Lower load(kN)	900	800
Upper load(kN)	1,500	1,200
Load range(kN)	600	400
Frequency(Hz)	3.0	3.2

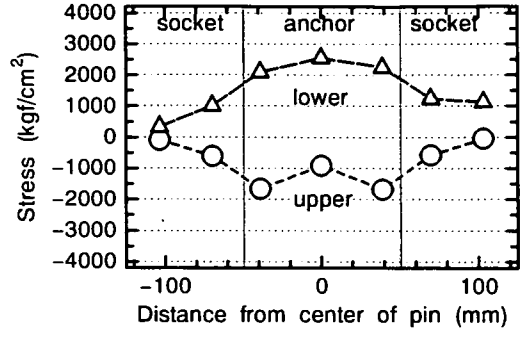

Fig.10 Measured stress at pin

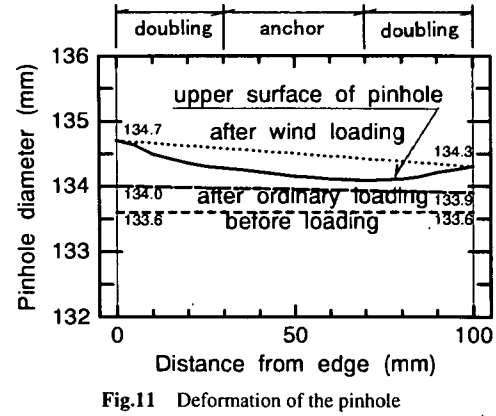

Fig.11 Deformation of the pinhole

(**Fig.14**). Displacements and rotations of all the nodes which are welded to the deck plate was fixed in all directions. The basic element used was a eight-node solid element. Fillet weld was modeled as a prism solid element. At interfaces between the anchor plate and doubling plates, coordinates of both nodes coincide for both plates indicating that all plates are separates from each other except at welds. The computer code used for analysis was NASTRAN version 68. Number of nodes is 3,568 and minimum size of element is 5mm. This element size is the same with the size of fillet weld. This size may not be small enough to evaluate the local stress due to the weld. However, since the main objective of analysis is to compare with the conventional

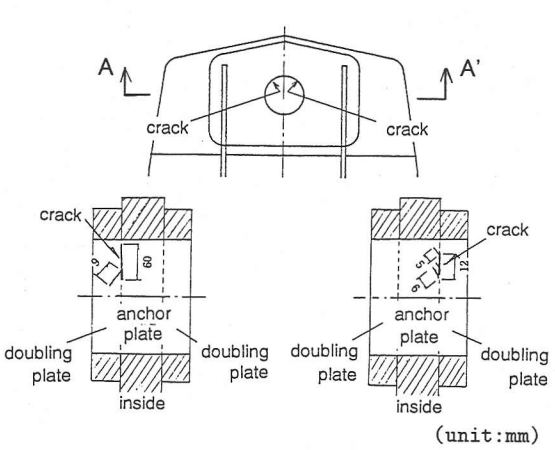

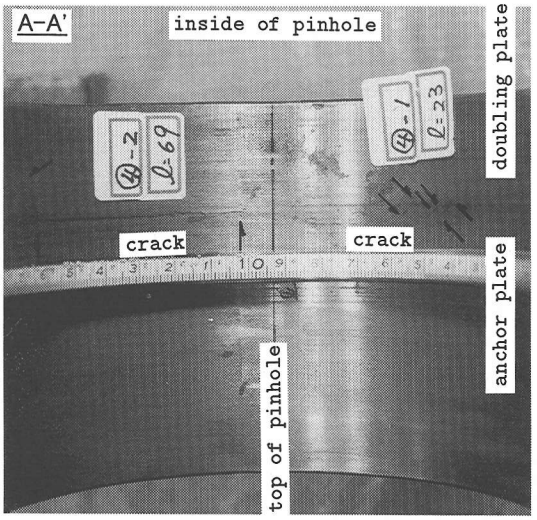

Fig.12 Fatigue cracks of pinhole

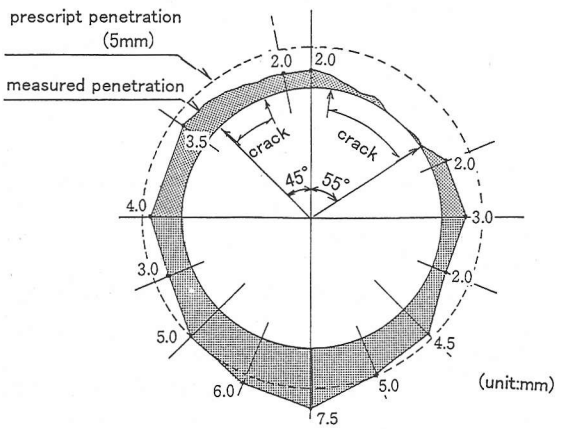

Fig.13 Penetration depth of seal weld

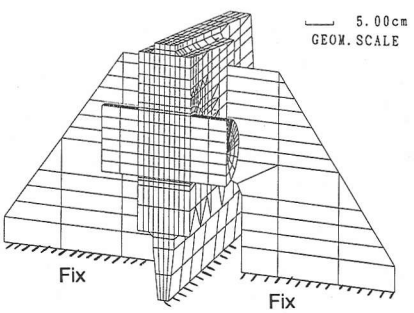

Fig.14 3-D Finite element model

design, the element size is considered to be sufficient.

Parameters considered in the analysis were; thickness of the anchor and doubling plates, diameter ratio of the pin to the pinhole, and effect of seal weld and loading condition as shown in **Table 3**.

In order to evaluate contact condition between the pin and the pinhole, a gap element was used at the interface attached to the pin's normal and tangential direction (**Fig.15**). The gap element transmits compression force only when the gap is computed less than zero. Axial rigidity of the gap element when closing was set 1.0E7kgf/cm, which is a sufficiently large value to avoid the entrenching of corresponding nodes. When the gap is opened, the axial rigidity is 10E-3kgf/cm. In this analysis, friction was not considered.

For the ordinary loading condition, vertical load was applied to the ends of the pin. For the wind loading condition, inclined rigid bars were connected to the ends of the pin to give an inclination angle.

(2) Deformation and stress distribution

Deformation of the anchor structure was shown in **Fig.16**. For analysis result of models without seal weld under the wind loading condition, a relative displacement was observed on the surface of the pin hole at boundary between the anchor and the doubling plates.

Principal stresses at the anchor structure under the ordinary loading condition are shown in **Fig.17**. The contact zone at the periphery of the pinhole was in compression, but other areas were in hoop tension. There was no significant difference in stress

Table 3 Analysis cases

Cases	Loading	Thickness of plates(mm)		Fillet weld	Seal weld
		Anchor plate	Doubling plate		
Case 1	Ordinary	40	30	○	○
Case 2	Wind	40	30	○	○
Case 3	Ordinary	40	30	○	−
Case 4	Wind	40	30	○	−
Case 5	Wind	10	45	○	○

Note : ○ means that the weld is performed.
Diameter ratio of the pin to the pinhole is 1.023.

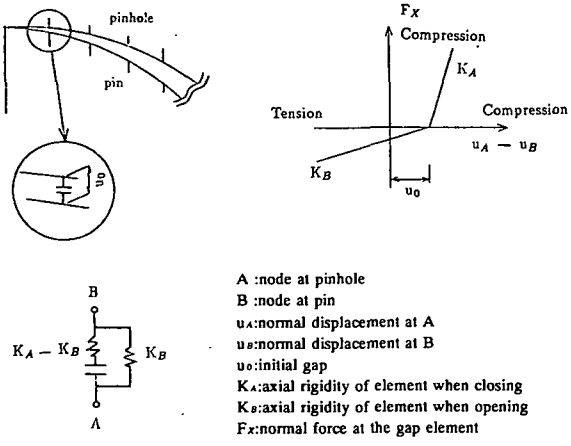

Fig.15 Gap element at interfaces between pin and pin hole

distribution between the anchor and doubling plates.

Fig.18 and **Fig.19** show stresses around the pinhole during the ordinary loading condition. Radial stress, σ_r, is higher at the outer face (section 1) than inside, meaning that higher bearing stress acts at edge elements of the doubling plate. Peripheral stress, σ_θ, concentrates at the outer surface of doubling plates. At the pin top, σ_θ stress at the outer surface is about twice higher than the anchor plate.

(3) Contact pressure distribution

a) Hertz's contact theory

Contact problem was treated classically by Hertz's theory[6]. It assumes that the contact area of two bodies is very small relative to their size, and the contact surface is remained elastic. Contact area and contact pressure are given by the following equations, assuming elastic modulus are the same for both contact bodies. This implies that the contact pressure is affected by diameter ratios of pin and pinhole.

$$a = \sqrt{\frac{4 \cdot P(1-\mu^2)}{\pi \cdot E} \cdot \left(\frac{d_1 \cdot d_2}{d_1 - d_2} \right)}$$

$$\sigma \max = \frac{2P}{\pi \cdot a}$$

Where α : contact peripheral length,
P : applied vertical load at pin,
d_1 : pinhole diameter,
d_2 : pin diameter,
E : modulus of elasticity,
μ : Poisson's ratio
and σ_{max} : maximum contact pressure.

b) Effect of diameter ratio on contact condition

Generally, diameter of a pinhole is determined by the site workability of inserting the pin into the pinhole. In the test, ratio of the pin and the pinhole diameters was set at 1.023, which is the Hertz's contact condition according to "Design Specifications for Highway Bridges" [7].

When the diameter ratio becomes smaller, i.e., diameter of the pinhole closes on that of the pin, the contact condition changes from Hertz's to plane condition.**Fig.20** shows that the changes of contact pressure as the diameters ratio changes from 1.02308 (diameters difference is 3mm) to 1.00769 (diameters difference is 1mm). The maximum stress reduces significantly as diameter ratio closes to 1.0. But even at the closest condition, the contact angle is still 58 degrees, which indicates that the design assumption of 90 degrees or even greater is not appropriate (see **Fig.21**).

c) Comparison

Fig.22 shows the contact pressure distribution along the axis of the pin. Under the ordinary loading condition, the computed peak contact pressure was 8,642kgf/cm^2 but the pressure decreased and leveled to 4,091kgf/cm^2 at the pin midpoint. The peak factor is 2.1.

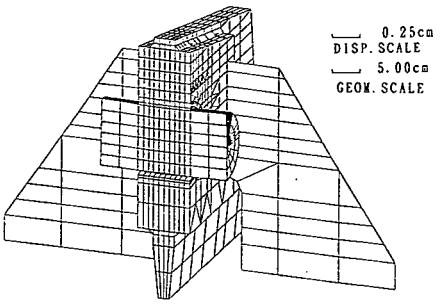

(a) Ordinary loading condition

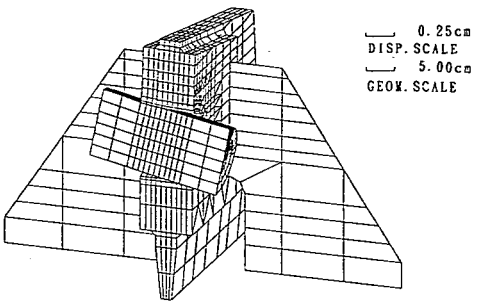

(b) Wind loading condition

Fig.16 Deformation of anchor structure

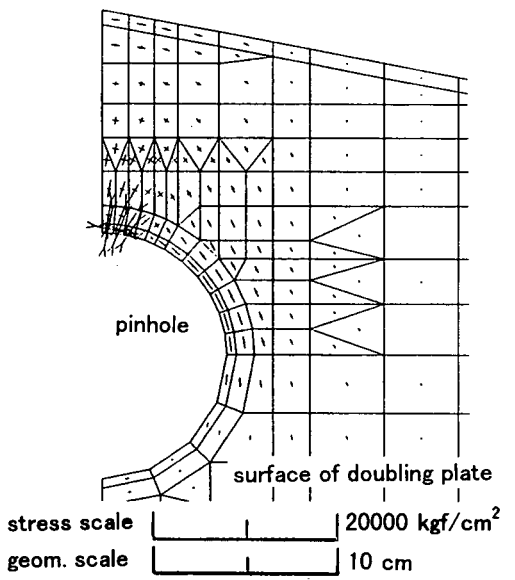

Fig.17 Computed major principal stress (Ordinary loading condition)

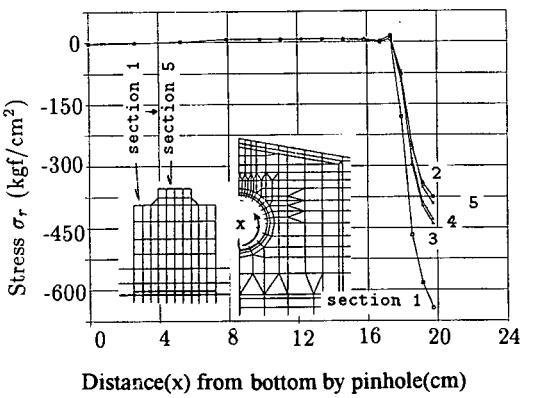

Fig.18 σ_r stress at top periphery (Ordinary loading condition)

But at the wind loading condition the computed peak pressure was 17,559kgf/cm^2. In a model without seal weld, the contact pressure distribution was discontinuous at the boundary of anchor and doubling plates.

Contact areas measured by the experiment, obtained from finite element analysis and Hertz's contact theory, are compared in **Table 4**. The experiment gives highest and finite element analysis and Hertz's theory is almost identical. The thickness of pressure scale paper (0.2mm) is considered to increase the apparent contact area.

During the wind loading condition, the maximum pressure at the edge of the pin was 17,559 kgf/cm^2, which exceeded the allowable bearing stress of steel SM490Y ($\fallingdotseq$7,000kgf/cm^2). In practical use, this high contact pressure is not considered to be a problem, because the area is very local and therefore contact pressure will be redistributed by yielding of the material.

Due to plastic deformation of the pinhole, contact area obtained from the experiment is considered to be much greater than the elastic finite element analysis.

(4) Pin bending moment

In conventional pin designing practice according to the "Design Specifications for Highway Bridges", a pin is modeled as a simply supported beam with a concentrated load acting at the mid-span (**Fig.23**). In this case the allowable stress is increased by 40% considering that the difference of support condition from the design assumption.

From the measured strains at seven different

Table 4 Comparison of contact areas, length, contact angle and maximum contact pressure (Ordinary loading condition)

Item		Ordinary loading condition			Wind loading condition	
		Experiment	3-D FEM	Hertz	Experiment	3-D FEM
Applied load (tf)		150			120	
Incline angle (deg)		0			3.2	
A (mm^2)		5,320	4,770	4,176	3,232	2,460
L (mm)		98	100	100	46	50
2a (mm)		54	58	44	96	46
θ (deg)		48	50	39	83	40
p (kgf/cm^2)	Edge	—	8,642	—	—	17,559
	Midpoint	—	4,100	4,420	—	—

A : contact area, L : contact length in pin's axial direction

2a : contact peripheral length

θ : angle of contact, p : contact pressure.

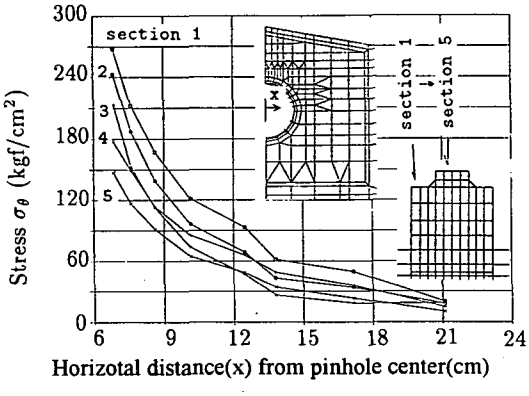

Fig.19 σ_θ stress at side periphery (Ordinary loading condition)

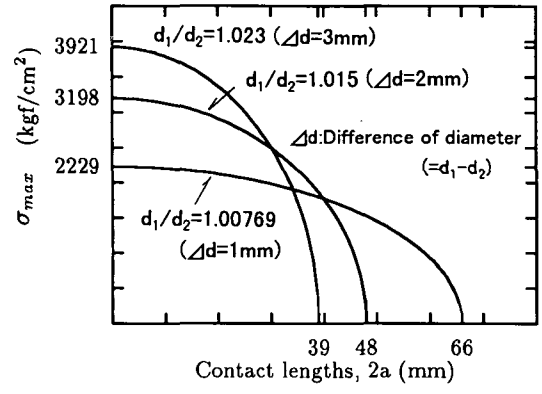

Fig.20 Contact pressure distribution with different diameter ratios (2-D FEM)

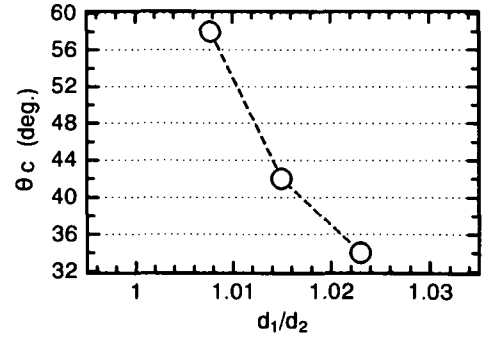

Fig.21 Change of contact area with different diameter ratios (2-D FEM)

locations at the top and bottom of the pin, bending moment was estimated. Also in the same way, the bending moment was calculated by integrating the elements stress obtained from finite element analysis.

As shown in **Fig.24**, the comparison between the conventional design method, finite element analysis, and the experiment, the measured pin bending moment is closer to uniform load condition in the conventional design method.

(5) Fatigue assessment and weld design

Cracks initiating at the seal weld of pinhole became the most serious problem because this type of cracks cannot be detected in practical operation.

The bearing stress is transmitted from the pin to the anchor and doubling plates individually but welds also interact especially under wind loading condition. When the seal weld is not performed, the stress carried by doubling plates eventually is transmitted to the anchor plate through fillet weld.

If the seal weld is performed, the stress is also carried by the seal weld and transmitted to the anchor plate. **Fig.25** shows stress distribution at welds.

Finite element analysis showed that the seal weld

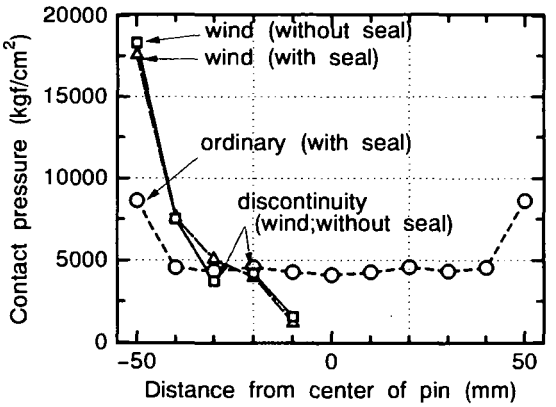

Fig.22 Computed contact pressure distribution (3-D FEM)

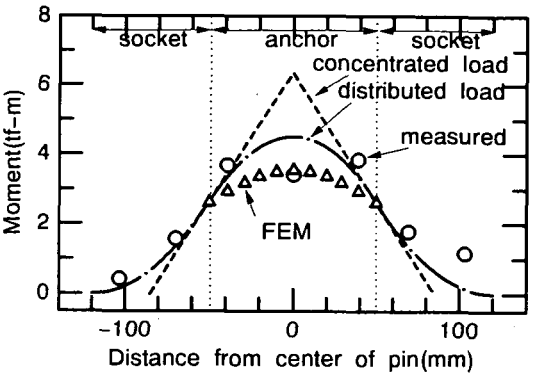

Fig.24 Comparison of pin bending moment between experiment, FEM, and conventional design method

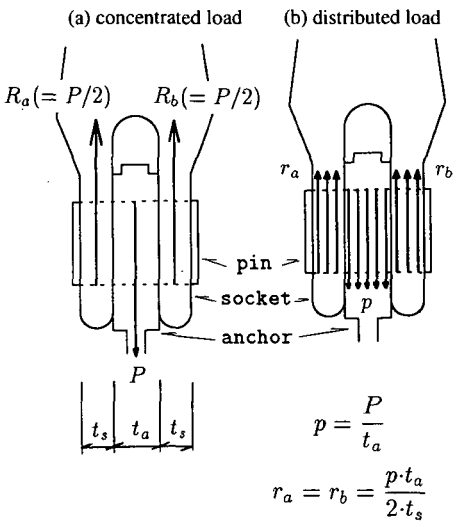

Fig.23 Assumptions for calculating pin bending moment

restricts the relative displacement between the anchor and doubling plates. Under the wind loading condition, the maximum von Mises stress at 5mm seal weld reached 3,713 kgf/cm^2 at 30 degrees measured from the top under the wind loading condition. When the seal weld is even smaller in size, it is estimated that higher stress concentration occurred at the seal weld. This stress concentration is considered to be the cause of the crack found in the experiment. From these analysis, it is revealed that the seal weld may become harmful when the seal weld is performed from the reason of corrosion protection of the pinhole. A sufficient weld penetration shall be remained in practice in order to prevent stress concentration.

However, when there is no seal weld but only fillet weld, stress at the fillet weld is only 4% greater than with the seal weld. This indicates that size of the fillet weld for doubling plates is not affected by the presence of seal weld. The size of the fillet weld, 9mm, in the analysis was determined from $\sqrt{2 \cdot t}$ where t is thickness of the thicker plate. The von Mises element center stress at the fillet weld is 2,321kgf/cm^2 (see **Table 5**) which is less than yield stress of SM490Y steel.

But in the previous report on cyclic test for a pin-connection anchor[5] showed that fatigue cracks occurred from fillet weld under wind loading condition. That specimen was different from this specimen structurally and in welding, i.e., there was not enough restriction of the out-of-plane bending and had no seal welding at the pinhole. The cause of cracks from the fillet weld in the previous test was probably due to the large out-of-plane bending deformation.

(6) Selection of thickness composition of anchor plate and doubling plate

Selection of the anchor and the doubling plates thickness composition is entrusted to the designer and it seems that there is no constraint. However, from the previous analysis it is estimated that during wind loading conditions where the compressive force acts eccentrically to the pinhole, the composition affects the stress distribution. Finite element analysis was then carried out by maintaining the same total thickness, i.e., a thicker anchor plate with a thinner doubling plate (40mm anchor plate and 30mm doubling plates : case A), as well as a thinner anchor plate with thicker doubling plates (10mm anchor plate and 45mm doubling plates : case B).

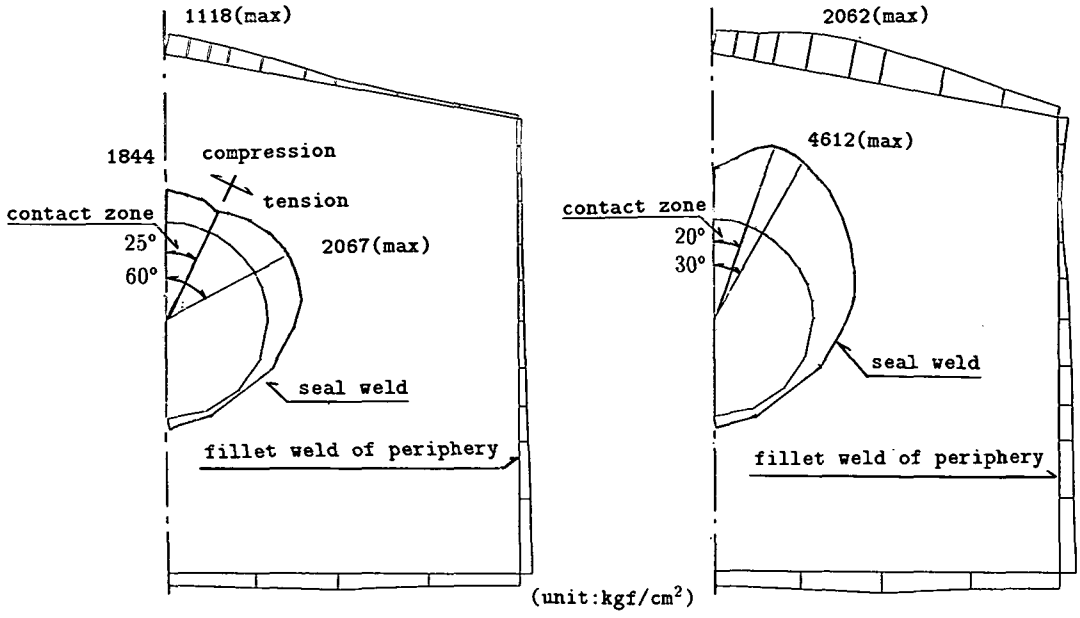

(a) Ordinary loading condition (b) Wind loading condition

Fig.25 Von Mises stress distribution between seal and fillet welds (node stress)

Table 5 Maximum von Mises stress at seal weld

(unit:kgf/cm²)

Loading and weld		$\sigma_{Mises,fillet}$	$\sigma_{Mises,seal}$
Ordinary	With seal weld	1,132	1,892
	Without seal weld	1,144	—
Wind	With seal weld	2,231	3,713
	Without seal weld	2,321	—

The maximum von Mises stress at welds were compared between the two cases. Stress at seal weld of case B was 26% less than that of case A, while stress at fillet weld was only 4% less. This indicates that when seal weld is performed, stress is carried more by doubling plate, but when seal weld is not performed, there seemed to be no significant difference between the two cases.

7. CONCLUSIONS

The following results were obtained from this study.

(1) Contact pressure distribution can be accurately calculated by FEM using a gap element at interfaces between the pin and the pinhole.

(2) Assuming pin contact angle of 90 degrees is not adequate for designing pin and anchor structures. Obtained relationship between diameter ratio between pin and pinhole as shown in **Fig.20** can be used. Minimizing diameters ratio of pin and pinhole effectively reduces the maximum contact pressure.

(3) Edge of the pinhole is highly pressured region which will be plastically deformed by an eccentric loading due to wind action.

(4) Pin bending moment is calculated using beam theory assuming the vertical load as uniform distribution along pin axis.

(5) Eccentric loading due to wind loading caused cracks from the seal weld. This crack extended along the seal weld line then to the anchor plate. Crack at the seal weld was initiating where penetration was small and contact pressure was highly concentrated.

(6) Under the wind loading condition, stress at the seal weld is extremely high with peak stress occurring at 30 degrees from top. This is a cause of the crack from the seal weld. In order to prevent this crack, the penetration of the seal weld should be sufficient.

(7) Stress carried by the fillet weld was not much affected by the presence of the seal weld at the

pinhole as shown in **Table 5**.
(8) Selection of plate thickness of anchor and doubling plates did not affect the stress distribution at welds.

ACKNOWLEDGMENT: The research was reviewed by The Committee on Steel Superstructure for the Honshu-Shikoku Bridges (Chairman: Dr. Fumio Nishino). Authors wish to acknowledge their beneficial discussions and suggestions.

REFERENCES

1) Cox,H.L. and Brown,A.F.C.: Stress of round Pins in holes, *Aeronaut.*Q.15, P.35, 1964
2) Suzuki,S., Goto,T. and Matsuura,S.: Stress Analysis and Design of Tie Plate used as a Bridge Restrainer, *Structural Engineering*, Vol.34A, 1988.3. (in Japanese)
3) Fatigue and Fracture in Steel Bridges, Case Studies. *John Willey & Sons, Inc.* 1984.
4) JSCE Research Committee on Superstructure of Honshu-Shikoku Bridges, *Committee Report on Superstructure of Honshu-Shikoku Bridges, Design Manual of Link Support for Suspension Bridges*, 1976.3. (in Japanese)
5) Ohashi,H., Fujii,Y., Ono,S. and Miki,C.: Force transmission mechanism and fatigue behavior of a pin-connection anchor for a long-span suspension bridge, *Journal of JSCE*, 1996.4. (in Japanese)
6) Hertz,H.: Über die Berührung fester elastischer Körper, *J. für die reine u. angew. Mathem., 92(1881) 156.*
7) Japan Road Association: Design Specifications for Highway Bridges (Steel Bridges), 1994.2. (in Japanese)

(Received September 3, 1996)

ダブリング補強された吊橋ハンガーピン定着部の接触挙動と溶接部の応力伝達

大橋治一・三木千壽・小野秀一

本論文は，箱桁を有する吊橋ハンガーのピン定着部における応力伝達および繰返し荷重を受ける場合の疲労に関して，実験および解析を行った結果を報告するものである．実物大の試験体を用いて静的載荷試験を行い，常時・暴風時におけるピン部の接触圧分布およびピンの応力を求めた．引き続き実施した繰返し載荷試験により，ピン孔に施工したシール溶接からきれつが発生することが明らかとなったため，これらに対する対策を提案した．最後に FEM 解析を行い実験結果と対比し，接触圧の分布および各溶接部の応力分担の状況を解明した．